JACS
JOURNAL OF THE AMERICAN CHEMICAL SOCIETY

COMMUNICATION

pubs.acs.org/JACS

High-Pressure Hydrothermal Crystal Growth and Multiferroic Properties of a Perovskite $YMnO_3$

Shintaro Ishiwata,*[,†,‡] Yusuke Tokunaga,[§] Yasujiro Taguchi,[‡] and Yoshinori Tokura[†,‡,§]

[†]Department of Applied Physics and Quantum-Phase Electronics Center (QPEC), University of Tokyo, Tokyo 113-8656, Japan

[‡]Cross-Correlated Materials Research Group (CMRG) and Correlated Electron Research Group (CERG), RIKEN ASI, Wako 351-0198, Japan

[§]Multiferroics Project, ERATO, Japan Science and Technology Agency (JST), c/o RIKEN, Wako 351-0198, Japan

ABSTRACT: Orthorhombic perovskites $RMnO_3$ are representative of spin-driven ferroelectrics. When the radius of the rare-earth ion R is smaller than that of Dy, for instance in $YMnO_3$, the orthorhombic phase becomes metastable at ambient pressure, which impedes the crystal growth; thus, the detailed magnetic and multiferroic properties of the metastable phase have not been characterized. In this work, we successfully obtained single crystals of orthorhombic $YMnO_3$ using quasi-hydrothermal conditions under a high pressure of 5.5 GPa. Magnetic and dielectric measurements under magnetic fields revealed that the magnetic ground state is the commensurate *E*-type antiferromagnetic, while a cycloidal spin phase likely coexists in the intermediate temperature range, which enhances the magnetoelectric response to external fields.

For next-generation memory devices, multiferroic materials are promising for the electric control of magnetic moments with low power consumption. Perovskite-type oxides, the most dominant minerals deep in the earth, have provided a rich variety of useful functions such as ferroelectricity and magnetism and moreover have been considered prime candidates for multiferroics.[1] Despite the tendency that ferroelectric and magnetic orders are exclusive of each other, their coexistence has been found in specific perovskites, which can be categorized into two different classes. Members of the first class, exemplified by $BiMO_3$ (M = Fe, $Ni_{0.5}Mn_{0.5}$),[2,3] show excellent ferroelectricity emerging independently from magnetic order. Members of the second class, exemplified by orthorhombic (*o*)-$RMnO_3$ (R = Tb−Lu)[4−9] and $GdFeO_3$,[10] show ferroelectricity induced by magnetic order and thus are often called spin-driven ferroelectrics.

The spin-driven ferroelectrics have attracted great attention since the discovery of the magnetically controllable ferroelectricity in *o*-$RMnO_3$ (R = Tb, Dy) with a perovskite-type structure.[4,11,12] The direction of the electric polarization **P** induced by an incommensurate cycloidal spin order through relativistic spin−orbit coupling can be switched by external magnetic fields,[13−15] but the *P* (=|**P**|) value of ∼0.1 $\mu C/cm^2$ is much smaller than that of the other class (typically several to several tens of $\mu C/cm^2$). On the other hand, it has been proposed that *P* is potentially gigantic in heavily distorted *o*-$RMnO_3$ (R = Ho−Lu, Y), which show a commensurate *E*-type antiferromagnetic order (Figure 1b). While the experimentally reported *P* in the *E*-type phase ranges from 0.025 to 0.5 $\mu C/cm^2$,[7−9] first-principles calculations considering the electron orbitals have suggested that

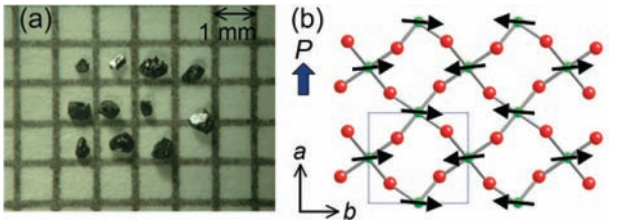

Figure 1. (a) Single crystals of perovskite-type $YMnO_3$. (b) Schematic crystal structure of the MnO_2 plane with an *E*-type antiferromagnetic order, viewed along the *c* axis.

P can be as large as 6 $\mu C/cm^2$.[16] Although the heavily distorted *o*-$RMnO_3$ with the *E*-type phase is a promising spin-driven ferroelectric material with potentially large *P*, the difficulty of crystal growth under high pressure has hampered the precise estimation of *P* and further studies of the multiferroic properties.

As a first step to clarify the multiferroic properties of the *E*-type phase, we prepared polycrystalline samples of *o*-$Eu_{1-x}Y_xMnO_3$ and *o*-$Y_{1-y}Lu_yMnO_3$ by a high-pressure technique and established the multiferroic phase diagram of *o*-$RMnO_3$ as a function of the radius of the R ion.[9] In view of the experimental fact that *o*-$YMnO_3$ is on the verge of the commensurate *E*-type phase adjacent to the *bc* cycloidal spin phase, both polycrystalline bulk and thin-film samples of *o*-$YMnO_3$ show a signature of the phase coexistence of these phases.[9,17,18] Previous neutron diffraction studies suggested that the magnetic ground state of *o*-$YMnO_3$ has an incommensurate spin arrangement, which is not compatible with the *E*-type phase.[19] In this work, we investigated a single crystal of *o*-$YMnO_3$ grown at high pressure under quasi-hydrothermal conditions, which exhibited multiferroic properties characteristic of the *E*-type phase coexisting with the minor cycloidal spin phase near the critical temperature.

Single crystals of *o*-$YMnO_3$ were grown under high pressure using the isomeric ambient-pressure phase with a hexagonal structure as a precursor.[20] A polycrystalline sample of hexagonal $YMnO_3$ was prepared by a solid-state reaction of a mixture of Y_2O_3 and Mn_2O_3 at 1300 °C in an ambient atmosphere. The thus-obtained precursor (150 mg) was mixed with KCl (30 mg) and water (10 mg), and the mixture was subjected to high-pressure, high-temperature conditions of 5.5 GPa and 1280−1100 °C for 2 h followed by quenching to room temperature. The sample was washed in distilled water to dissolve KCl.

Received: June 10, 2011
Published: August 09, 2011

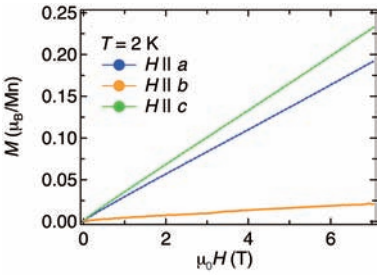

Figure 2. Magnetization curves of perovskite-type $YMnO_3$ with external magnetic fields applied along the *a*, *b*, and *c* axes.

As shown in Figure 1a, black crystals of *o*-$YMnO_3$ with the largest dimensions of 0.5 mm × 0.4 mm × 0.4 mm were obtained, and the crystal orientation was determined by Laue X-ray diffraction. The shiny facet corresponds to the *c* plane in the *Pbnm* setting. The lattice parameters of the single crystal *o*-$YMnO_3$ [*a* = 5.261(3) Å, *b* = 5.843(4) Å, *c* = 7.356(5) Å as determined by a triple-axis diffractometer] were close to those of the polycrystalline *o*-$YMnO_3$ [*a* = 5.258(1) Å, *b* = 5.845(1) Å, *c* = 7.356(1) Å].[9] Detailed structure analyses of both the paraelectric and ferroelectric phases was reported elsewhere.[21] Although the formation of twin domain boundaries along [110] or [1$\bar{1}$0] in the *c* plane was confirmed using a polarized light microscope, one of them predominantly occupies the crystals. We also tried crystal growth of *o*-$YMnO_3$ using KCl as a flux under the same pressure and temperature conditions without adding water. However, the obtained sample was in the polycrystalline form of *o*-$YMnO_3$. Since the melting point of KCl increases drastically upon application of pressure (from 780 °C at ambient pressure to 1450 °C at 4 GPa),[22] a small amount of supercritical water is necessary to reduce the melting point of KCl. Recently, single crystals of *o*-$HoMnO_3$ less than 30 μm in size were grown under conventional hydrothermal conditions, but the crystals were too small for the multiferroic properties of the *E*-type phase to be studied.[23]

For measurements of the dielectric constant and the electric polarization *P*, an LCR meter and an electrometer were used, respectively. The applied electric field **E** was perpendicular to the *c* axis and made an angle θ of 33.5° with the *a* axis. Since the exchange striction working in the *E*-type phase was expected to yield *P* along the *a* axis, the raw polarization data P_{raw} were multiplied by 1/cos θ (≈1.2) for calibration. As a poling procedure, *E* (=|**E**|) of 10 kV/cm was applied at 35 K, followed by cooling to 2 K. The displacement current, which was measured as a function of temperature as *T* increased at a rate of 5 K/min, was integrated as a function of time to obtain *P*. External magnetic fields were applied during the poling and measuring procedures. Magnetization was measured using a SQUID magnetometer.

Figure 2 shows magnetization curves of *o*-$YMnO_3$ along the respective crystallographic axes at 2 K. The *b*-axis component shows a minimal response compared with the *a*- and *c*-axis ones and is consistent with the proposed spin structure of the *E*-type phase having spins nearly parallel to the *b* axis. Recent studies based on terahertz spectroscopy and model calculations have suggested that the Dzyaloshinskii−Moriya interaction and the single-ion anisotropy yield staggered spin canting that deviates slightly from the *b* axis toward the *a* axis (see Figure 1b).[17,24] The slightly smaller magnetization along the *a* axis than along the *c* axis reflects the staggered antiferromagnetic component along the *a* axis.

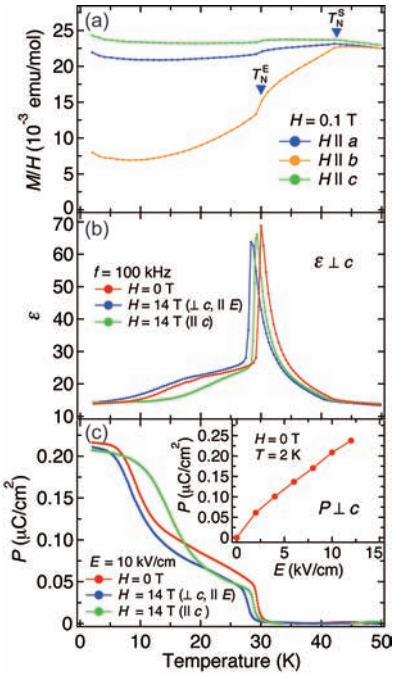

Figure 3. Temperature dependence of (a) magnetic susceptibility (data taken from ref 21), (b) dielectric constant at a frequency of 100 kHz, and (c) electric polarization for a perovskite-type $YMnO_3$ crystal. All of the measurements were performed with increasing temperature. The magnetization data were measured under a magnetic field of 0.1 T applied along each crystallographic axis, while the dielectric constant and polarization data were measured under zero magnetic field or magnetic fields applied along the *c* axis (green curve) or the direction of the electric field **E** (blue curve). The inset in (c) shows the poling electric field dependence of the polarization at 2 K. For higher poling fields, the sample breaks down.

As shown by the temperature dependence of the magnetic susceptibility (Figure 3a), the phase transitions from the paramagnetic phase to the sinusoidal antiferromagnetic phase and from the sinusoidal phase to the *E*-type antiferromagnetic phase were observed at T_N^S = 42 K and T_N^E = 30 K, respectively. The ferroelectric transition induced by the *E*-type spin order was clearly seen in the dielectric and polarization measurements (Figure 3b,c). The small kink in the dielectric constant (ε) at 42 K corresponds to a transition between the paramagnetic and sinusoidal antiferromagnetic phases. Upon the *E*-type antiferromagnetic ordering at 30 K, the temperature dependences of ε and *P* show a sharp kink and a sudden increase, respectively, which are characteristic of the (weakly) first-order ferroelectric transition. As the temperature decreases below T_N^E, *P* shows a stepwise increase (as observed for the polycrystalline sample) and reaches ~0.22 μC/cm^2 at 2 K, which is much larger than the value reported for the polycrystalline sample.[9] Notably, *P* at 2 K does not saturate with increasing *E* up to 12 kV/cm (Figure 3c inset), while the sample breaks down for higher *E*. Corresponding to the stepwise increase in *P*, ε shows a change in the slope at ~15 K. Theoretical analysis of the magnetic phase diagram of *o*-$RMnO_3$ has suggested that the coexistence of the commensurate *E*-type phase and the incommensurate cycloidal spin phase may be realized in *o*-$YMnO_3$ in the intermediate temperature range just

dx.doi.org/10.1021/ja205408m |*J. Am. Chem. Soc.* 2011, 133, 13818–13820

below T_N^E.[17,25] The temperature-dependent volume fraction of the *bc* cycloidal spin phase could be the origin of the nonmonotonic temperature profile of the observed *P*, such as the suppression of *P* over the temperature range 10−30 K.

Under an external magnetic field *H* of 14 T applied along either the *c* axis or the direction of **E** ($\perp c$), T_N^E decreases by 1−2 K, as shown in Figure 3a,b. The magnetocapacitance [defined a $\Delta\varepsilon(H)/\varepsilon(0)$] is ∼145% at 28.3 K for **H** perpendicular to the *c* axis. When **H** is parallel to the *c* axis, both ε and *P* show significant changes over the temperature range 10−20 K, unlike the case of **H** perpendicular to the *c* axis. Given the presence of the minority *bc* cycloidal spin phase, which is unstable when **H** is parallel to the *c* axis, the enhancement of *P* in the range 10−20 K for **H** parallel to the *c* axis can be ascribed to the **H**-induced replacement of the cycloidal spin phase with the *E*-type phase. *P* at 2 K is almost unchanged when **H** is applied along either direction, reflecting the predominance of the *E*-type phase over the *bc* cycloidal spin phase at the lowest temperature.

In summary, we have succeeded in growing single crystals of *o*-$YMnO_3$ with the use of quasi-hydrothermal conditions under high pressure and revealed giant magnetocapacitance and magnetoelectric effects. On the basis of the anisotropic features of the magnetic and dielectric responses, the *E*-type antiferromagnetic state with the spin directions parallel to the *b* axis is clearly assigned to a major source of the *a*-axis spontaneous polarization. Although a spin arrangement in the *E*-type phase is robust against the application of **H**, the magnetoelectric responses are likely enhanced by the coexistence of the minor phase with the *bc* cycloidal spin order.

AUTHOR INFORMATION

Corresponding Author
ishiwata@ap.t.u-tokyo.ac.jp

ACKNOWLEDGMENT

The authors thank D. Okuyama, T. Arima, and M. Mochizuki for fruitful discussions. This research was funded by the Japan Society for the Promotion of Science (JSPS) through the "Funding Program for World-Leading Innovative R&D on Science and Technology (FIRST Program)" initiated by the Council for Science and Technology Policy (CSTP).

REFERENCES

(1) Khomskii, D. I. *J. Magn. Magn. Mater.* **2006**, *306*, 1.
(2) Wang, J.; Neaton, J. B.; Zheng, H.; Nagarajan, V.; Ogale, S. B.; Liu, B.; Viehland, D.; Vaithyanathan, V.; Schlom, D. G.; Waghmare, U. V.; Spaldin, N. A.; Rabe, K. M.; Wuttig, M.; Ramesh, R. *Science* **2003**, *299*, 1719.
(3) Azuma, M.; Takata, K.; Saito, T.; Ishiwata, S.; Shimakawa, Y.; Takano, M. *J. Am. Chem. Soc.* **2005**, *127*, 8889.
(4) Kimura, T.; Goto, T.; Shintani, H.; Ishizaka, K.; Arima, T.; Tokura, Y. *Nature* **2003**, *426*, 55.
(5) Kimura, T.; Lawes, G.; Goto, T.; Tokura, Y.; Ramirez, A. P. *Phys. Rev. B* **2005**, *71*, No. 224425.
(6) Hemberger, J.; Schrettle, F.; Pimenov, A.; Lunkenheimer, P.; Ivanov, V. Yu.; Mukhin, A. A.; Balbashov, A. M.; Loidl, A. *Phys. Rev. B* **2007**, *75*, No. 035118.
(7) Lorenz, B.; Wang, Y.-Q.; Chu, C.-W. *Phys. Rev. B* **2007**, *76*, No. 104405.
(8) Pomjakushin, V. Yu.; Kenzelmann, M.; Dönni, A.; Harris, A. B.; Nakajima, T.; Mitsuda, S.; Tachibana, M.; Keller, L.; Mesot, J.; Kitazawa, H.; Takayama-Muromachi, E. *New J. Phys.* **2009**, *11*, No. 043019.
(9) Ishiwata, S.; Kaneko, Y.; Tokunaga, Y.; Taguchi, Y.; Arima, T.; Tokura, Y. *Phys. Rev. B* **2010**, *81*, No. 100411.
(10) Tokunaga, Y.; Furukawa, N.; Sakai, H.; Taguchi, Y.; Arima, T.; Tokura, Y. *Nat. Mater.* **2009**, *8*, 558.
(11) Kenzelmann, M.; Harris, A. B.; Jonas, S.; Broholm, C.; Schefer, J.; Kim, S. B.; Zhang, C. L.; Cheong, S.-W.; Vajk, O. P.; Lynn, J. W. *Phys. Rev. Lett.* **2005**, *95*, No. 087206.
(12) Yamasaki, Y.; Sagayama, H.; Goto, T.; Matsuura, M.; Hirota, K.; Arima, T.; Tokura, Y. *Phys. Rev. Lett.* **2007**, *98*, No. 147204.
(13) Katsura, H.; Nagaosa, N.; Balatsky, A. V. *Phys. Rev. Lett.* **2005**, *95*, No. 057205.
(14) Mostovoy, M. *Phys. Rev. Lett.* **2006**, *96*, No. 067601.
(15) Sergienko, I. A.; Dagotto, E. *Phys. Rev. B* **2006**, *73*, No. 094434.
(16) Picozzi, S.; Yamauchi, K.; Sanyal, B.; Sergienko, I. A.; Dagotto, E. *Phys. Rev. Lett.* **2007**, *99*, No. 227201.
(17) Mochizuki, M.; Furukawa, N. *Phys. Rev. Lett.* **2010**, *105*, No. 037205.
(18) Nakamura, M.; Tokunaga, Y.; Kawasaki, M.; Tokura, Y. *Appl. Phys. Lett.* **2011**, *98*, No. 082902.
(19) Muñoz, A.; Alonso, J. A.; Casais, M. T.; Martínez-Lope, M. J.; Martínez, J. L.; Fernández-Díaz, M. T. *J. Phys.: Condens. Matter* **2002**, *14*, 3285.
(20) Uusi-Esko, K.; Malm, J.; Imamura, N.; Yamauchi, H.; Karppinen, M. *Mater. Chem. Phys.* **2008**, *112*, 1029.
(21) Okuyama, D.; Ishiwata, S.; Takahashi, Y.; Yamauchi, K.; Picozzi, S.; Sugimoto, K.; Sakai, H.; Takata, M.; Shimano, R.; Taguchi, Y.; Arima, T.; Tokura, Y. *Phys. Rev. B* **2011**,*84*, No.054440.
(22) Pistorius, C. W. F. T. *J. Phys. Chem. Solids* **1965**, *26*, 1543.
(23) Chen, Y.; Yuan, H.; Li, G.; Tian, G.; Feng, S. *J. Cryst. Growth* **2007**, *305*, 242.
(24) Takahashi, Y.; Ishiwata, S.; Miyahara, S.; Kaneko, Y.; Furukawa, N.; Taguchi, Y.; Shimano, R.; Tokura, Y. *Phys. Rev. B* **2010**, *81*, 100413.
(25) Dong, S.; Yu, R.; Yunoki, S.; Liu, J.-M.; Dagotto, E. *Phys. Rev. B* **2008**, *78*, No. 155121.